HHS Public Access

Author manuscript

Dev Neurobiol. Author manuscript; available in PMC 2017 October 01.

Published in final edited form as:

Dev Neurobiol. 2016 October ; 76(10): 1092–1110. doi:10.1002/dneu.22377.

Drebrin Coordinates the Actin and Microtubule Cytoskeleton During the Initiation of Axon Collateral Branches

Andrea Ketschek[1], **Mirela Spillane**[1], **Xin-Peng Dun**[2], **Holly Hardy**[3], **John Chilton**[3], and **Gianluca Gallo**[1,*]

[1]Shriners Hospitals Pediatric Research Center, Temple University School of Medicine, Department of Anatomy and Cell Biology, 3500 N. Broad St, Philadelphia PA 19140

[2]Peninsula Schools of Medicine and Dentistry, University of Plymouth, Plymouth Science Park, Research Way, Plymouth PL6 8BU, United Kingdom

[3]University of Exeter Medical School, Wellcome Wolfson Medical Research Centre, RILD Building, Barrack Road, Exeter EX2 5DW, United Kingdom

Abstract

Drebrin is a cytoskeleton-associated protein which can interact with both actin filaments and the tips of microtubules. Its roles have been studied mostly in dendrites, and the functions of drebrin in axons are less well understood. In this work we analyzed the role of drebrin, through shRNA-mediated depletion and over-expression, in the collateral branching of chicken embryonic sensory axons. We report that drebrin promotes the formation of axonal filopodia and collateral branches in vivo and in vitro. Live imaging of cytoskeletal dynamics revealed that drebrin promotes the formation of filopodia from precursor structures termed axonal actin patches. Endogenous drebrin localizes to actin patches and depletion studies indicate that drebrin contributes to the development of patches. In filopodia, endogenous drebrin localizes to the proximal portion of the filopodium. Drebrin was found to promote the stability of axonal filopodia and the entry of microtubule plus tips into axonal filopodia. The effects of drebrin on the stabilization of filopodia are independent of its effects on promoting microtubule targeting to filopodia. Inhibition of myosin II induces a redistribution of endogenous drebrin distally into filopodia, and further increases branching in drebrin overexpressing neurons. Finally, a 30 minute treatment with the branch inducing signal nerve growth factor increases the levels of axonal drebrin. The current study determines the specific roles of drebrin in the regulation of the axonal cytoskeleton, and provides evidence that drebrin contributes to the coordination of the actin and microtubule cytoskeleton during the initial stages of axon branching.

INTRODUCTION

Axon branching is a fundamental mechanism in the development and repair of neuronal circuitry (Gibson and Ma, 2011; Onifer et al., 2011). The generation of axon collateral branches involves the coordinated reorganization of the actin filament and microtubule cytoskeleton (Dent and Kalil, 2001; Gallo, 2011; Kalil and Dent, 2014). However, how

*Corresponding author: gianluca.gallo@temple.edu, Ph: 215 926 9362, Fax: 215 926 9325.

cytoskeletal dynamics are orchestrated remains poorly understood. Branches are initiated as actin filament based filopodial protrusions along the axon shaft, which subsequently become invaded by axonal microtubules and mature into a branch resembling the parent axon. The emergence of axonal filopodia along embryonic sensory axons is preceded by precursor structures termed actin patches (Gallo, 2013). Actin patches are transient accumulations of actin filaments along the axon shaft which represent a network of filaments (Spillane et al., 2011). The shafts of filopodia, which contain aligned and bundled actin filaments, emerge from axonal actin patches (Spillane et al., 2011). Localized microdomains of phosphoinositide 3-kinase (PI3K) signaling along the axon determine the sites of formation and duration of the actin patches (Ketschek and Gallo, 2010). The formation of actin patches is in part dependent on the activity of the actin nucleating Arp2/3 complex (Spillane et al., 2011). Cortactin and septin 6 contribute to the emergence of filopodia from patches (Mingorance-Le Meur and O'Connor, 2009; Hu et al., 2012; Spillane et al., 2012), which is negatively controlled by RhoA-kinase and myosin II (Loudon et al., 2006). The mechanism that controls the targeting of microtubules into filopodia is less understood, but septin 7 accumulates at the proximal-most base of filopodia and promotes the targeting of axonal microtubules into filopodia independent of the regulation of filopodia (Hu et al., 2012). The formation of branches is under regulation by extracellular signals which can either promote or impair branching (Gibson and Ma, 2011). NGF promotes sensory axon branching through the regulation of both the actin and microtubule cytoskeleton (Spillane et al., 2011, 2012, 2013). In this investigation we sought to further understand the molecular mechanism underlying the integration of the actin filament and microtubule cytoskeleton during axon branching.

We considered a role for drebrin among the host of proteins which have the potential to directly bind both the axonal actin filament and microtubule cytoskeleton (Houseweart and Cleveland, 1999; Dent and Gertler, 2003; Rodriguez et al., 2003; Goryunov et al., 2010; Fukushima et al., 2011; Huber et al., 2014; Villarroel-Campos D and Gonzalez-Billault, 2014). Drebrin is a neuronally expressed actin filament binding protein that has been involved in the regulation of neuronal morphology (Dun and Chilton, 2010; Dun et al., 2012). Drebrin can bundle actin filaments (Worth et al., 2013), regulate the binding of additional actin binding proteins to filaments (reviewed in Dun and Chilton, 2010) and importantly can also directly associate with microtubule plus tips through the end binding (EB) proteins (Geraldo et al., 2008; Bazellières et al., 2012). While there are multiple possible molecules involved in branching that have the potential to bind actin filaments and microtubules and thus serve as coordinators between these two cytoskeletal systems, no study to date has simultaneously addressed the role of any of these molecules in the regulation of the both the actin and microtubule cytoskeleton during branching. Collectively, this study identifies drebrin as the first known individual coordinator of the actin and microtubule axonal cytoskeleton during axon branching.

METHODS

Cell culture and transfection

Chicken embryonic day 7 (E7) DRG neurons were cultured as explants or dissociated cells using previously described protocols (Lelkes et al., 2006; Ketschek and Gallo, 2010). Briefly, cells were cultured in defined F12H medium with additives and 20ng/ml NGF (Invitrogen) on glass coverslips coated with 25μg/ml laminin (Invitrogen). For experiments investigating the effects of NGF on drebrin protein levels, cells were cultured in F12H medium in the absence of NGF. Cultures were treated with 40 ng/mL NGF 24 hours after plating as described in the Results. All transfections were successfully completed using 10 μg of the plasmid and the Amaxa Biosystems Nucleofector II setting G-013. The following plasmids, YFP-Drebrin E1, RFP-Drebrin E1, Drebrin 308 shRNA-GFP, and Drebrin 308 scrRNA-GFP (scrambled control) were previously described in Dun et al. (2012). Additional plasmids used, eYFP-β actin, mCherry-beta actin, and GFP/mCherry-EB3, were described in Ketschek et al (2007, 2010).

In ovo electroporation

In ovo electroporation and *ex vivo* imaging was performed as previously described by Spillane et al (2011). Briefly, lumbosacral chicken embryo DRGs were electroporated *in ovo* at E3 using a CUY-21SC electroporator (Nepa Gene) equipped with 3 mm L-shaped gold tip electrodes (Harvard Apparatus). YFP-Drebrin E1 or GFP-control expression vectors were injected (0.1–0.15 μg/μl) into the lumen of the neural tube and electrodes were placed at the level of the lumbosacral enlargement. Five 50 ms 50 V pulses were applied at a rate of 1 pulse per second. Embryos were later removed from the eggs at E7 and the entire spinal cord, caudal to the first thoracic segment was dissected out. The cord was then divided into two halves and immediately placed on a video-imaging dish with 20 μl of culturing medium for imaging. Imaging was performed using a 100x objective on a Zeiss 200 m inverted microscope equipped with an Orca-ER camera (Hamamatsu).

Reagents

NGF was obtained from R & D Systems and used at a final concentration of 40 ng/ml. Blebbistatin was obtained from Toronto Research Chemicals in North York, Ontario Canada and used at a final concentration of 50 μM. Vinblastine was purchased through Sigma and used at a final concentration of 3 nM. Cycloheximide was purchased from Sigma and dissolved in DMSO, and used at a final concentration of 35 μM.

Immunohistochemistry

E7 embryos were decapitated and fixed in 4% paraformaldehyde before embedding in 20% gelatine dissolved in phosphate-buffered saline (PBS). Sections were cut on a vibratome in the transverse plane of the embryo at a thickness of 50μm. The sections were blocked in PBS containing 10% heat-inactivated sheep serum (HISS) and 0.5% Triton X-100, primary antibodies to drebrin (mouse monoclonal M2F6, 1:100; Abcam) and neurofilament medium chain (rabbit polyclonal AB1987,1:100; Chemicon) and secondary antibodies (Alexa488 and Alexa568 conjugated, 1:400; Molecular Probes, Invitrogen) were added in the blocking

medium. Samples were washed in PBS containing 1% HISS and 0.5% Triton X-100, after incubation with secondary antibodies, DAPI was applied (conc.; Molecular Probes, Invitrogen) before washing three times and mounting in FluorSave medium (Calbiochem).

Immunocytochemistry and quantification of intensities

Cultures were fixed using one of the two following protocols; (1) with a final concentration of 4% paraformaldehyde (PFA; Electron Microscopy Sciences) containing 5% sucrose or (2) with a final concentration of 0.25% glutaraldehyde. To detect the distribution of drebrin along axons, we used a mouse antibody to drebrin (1:1000; M2F6-abcam). Microtubules were stained using a FITC-conjugated anti-α-tubulin monoclonal antibody (DM1A clone, 1:100; Sigma) and actin filaments were stained using rhodamine phalloidin or Alexa488 phalloidin (8 μl/100 μl of staining solution; Invitrogen). Blocking and application of antibodies was performed with PBS supplemented with 10% goat serum and 0.1% triton X-100 (GST). Samples were washed three times with PBS between treatment of primary and secondary antibodies. Coverslips were mounted using Vectashield (Vector Laboratories).

To measure the amount of drebrin in axons we followed our previously published protocols (e.g., Spillane et al., 2012). We used cultures processed and stained in parallel with all images acquired during the same microscopy session using image acquisition parameters that yielded no saturated pixels. The total amount of drebrin in the distal 50 μm of the axons was then determined by multiplying the mean background subtracted staining intensity of drebrin in the defined region of interest by the total pixel count of the area. This method has previously been used to analyze the intra-axonal protein synthesis dependent levels of cortactin, Arp2 and WAVE1 which are increased by NGF treatment, unlike the total levels of α-tubulin or microtubule associated protein 1B which are not affected by NGF (Spillane et al., 2012; Ketschek et al., 2015).

For consideration of the effectiveness of shRNA-mediated depletion of drebrin scrambled and drebrin shRNA cultures were processed in parallel and imaged during the same imaging session using identical parameters. The exposure was first determined by imaging samples that had been stained with the secondary antibody but omitted the primary, thus only providing non-specific secondary antibody staining. The exposure was set so that in these samples no signal was detectable.

Western blotting

Dorsal root ganglia and dorsal spinal cords were dissected from chick embryos at the relevant developmental stages and homogenised in lysis buffer (1% Triton X-100, 10% Glycerol, 25 mM HEPES, 5 mM EDTA, 1 mM $MgCl_2$, 2 mM PMSF). Equal amounts of cleared lysates were fractionated by SDS-PAGE using 10% polyacrylamide gels and transferred to polyvinylidene membranes (Immobulon, Merck Millipore). PVDF membranes with bound proteins were blocked (TBS, 0. 1% Tween, 5% non-fat dry milk) for one hour at room temperature, incubated overnight at 4°C with anti-drebrin M2F6 (1:1000), followed by secondary antibodies conjugated to horseradish peroxidase (1:5000; Sigma-Aldrich) and visualised with SuperSignal West Femto enhanced chemiluminescent reagent (Thermo Fisher Scientific Inc.).

Live imaging

All imaging, data acquisition, and analysis were performed using a Carl Zeiss 200M microscope equipped with an Orca ER camera (Hamamatsu) (same imaging setup as described previously by Loudon et al., 2006). Live and fixed cultures were observed using a 100x, 1.3 numerical aperture objective for both phase and fluorescence microscopy. Quantitative analysis of patches was performed using the protocols previously described by Loudon et al., 2006 and Ketschek and Gallo, 2010. To measure β-actin patch formation and lifespans, images were acquired using 6 s interframe intervals for 5 min. Time-lapse and quantitative analysis was performed using the interactive measurement module of the AxioVision Software.

Analysis of filopodia and branches

Branches were determined as previously described using morphological criteria (Spillane et al., 2012, 2013). Briefly, branches were defined by (1) thickening and phase-contrast darkening of the filopodium and (2) the emergence of protrusive activity from the otherwise linear structure of the filopodium. To analyze filopodia dynamics in the distal 50 μm of the axon excluding the growth cone (defined as the most distal 10 μm), images were acquired using 10 sec interframe intervals for 5 minutes. The lifespan of each filopodia (time at which filopodia appear to when the filopodia is retracted back into the axon shaft) was recorded. Pre-existing filopodia were also categorized as dynamic (any extension or retraction during the 5 minute time frame) or non-dynamic (no extension or retraction within the 5 minute time frame). All analysis of filopodia and branches was performed at 100x a magnification better suited for the analysis of these structures. Only axons that were not contacted by, and thus possibly fasciculated with, other axons were considered for analysis.

Statistical analysis

Data were analyzed using Instat 3 software (GraphPad Inc.). The software automatically uses the Kolmogorov-Smirnov test to determine the normalcy of data sets. If any data set in an experimental design was not normal then non-parametric analysis was performed. For these data sets, the data presented in the text include the mean and the median with the standard error of measurement (mean/median ± SEM). Parametric data sets are presented as means and standard error of measurements. If all sets were normally distributed then Welch t-tests were used, with paired test used for pre-post experimental designs. Categorical data sets were analyzed through the Fischer's test using the raw categorical data, and data are presented as percentages in graphs.

RESULTS

Expression of Drebrin in dorsal root ganglia in vivo

Drebrin is expressed in the growth cones of cultured dorsal root ganglion neurons at E7 (Dun et al. 2012) but it is unknown whether this reflects its expression in vivo at the same developmental stage. We performed fluorescent immunohistochemistry on transverse sections of E7 embryos and observed prominent localization of drebrin to the processes of sensory neurons as they invade the neural tube and in the dorsal columns along which they

send their projections (Figure 1A–D). Drebrin occurs in two embryonic isoforms and one adult form, which are developmentally regulated by alternative splicing of mRNA (Kojima et al. 1993). The corresponding changes in the protein isoforms in DRGs have not been fully described, and no distinguishing antibodies are available for immunohistochemical investigation although the individual isoforms can be separated by size on a Western blot. We confirmed that at E5, in dorsal root ganglia and the dorsal columns of the spinal cord, the E1 isoform predominates with low levels of the larger E2 isoform present (Figure 1E). At E7 there is near parity of expression, and by E9 the E2 isoform is the major form present in these tissues (Figure 1E). The A isoform is not present at these stages although it can be distinguished as a third, larger band in the retina at E9 (data not shown). These data demonstrate that the in vivo expression profile of drebrin is maintained in culture and that previously reported changes in RNA production (Kojima et al. 1993) are mirrored at the protein level.

Drebrin positively regulates the number of axonal filopodia and collateral branches along the axons of sensory neurons

Dun et al. (2012) reported that drebrin levels positively regulate the number of axonal filopodia and branches generated by oculomotor neurons in vivo. However, the specific contributions of drebrin to the underlying cytoskeletal dynamics have not been elucidated. To further understand the role of drebrin in axon branching, we investigated the underlying mechanisms by which drebrin influences the emergence of axonal filopodia and branches, the first step of a collateral branch using chicken embryonic sensory neurons. We first sought to confirm the previously described role of drebrin in the regulation of axonal filopodia and branches in embryonic chicken sensory dorsal root ganglion neurons *in vivo*. Drebrin is expressed in embryonic (E) and adult (A) forms (Dun and Chilton, 2010). As the current study focuses on embryonic neurons we used drebrin E1 for our studies. Dorsal root ganglion sensory neurons were transfected *in ovo* with YFP- drebrin E1 using previously established electroporation techniques (Spillane et al., 2011, 2012, 2013). The morphology of YFP-drebrin E1 expressing axons in the dorsal columns of the living spinal cord was imaged using an acute embryonic day (E) 7 spinal cord explant system as previously reported and similarly analyzed for the presence of axonal filopodia and branches using morphological characteristics (Spillane et al., 2011, 2012, 2013). Axons expressing drebrin E1 were more complex compared to the relatively simple morphology displayed by control axons expressing GFP, exhibiting many filopodia and branches compared to GFP control axons (Fig. 1A). One or more branches were present along the distal axons of 19% (n=53) and 57% (n=47) of GFP and YFP-drebrin E1 expressing neurons respectively ($p<0.0001$, Fisher's exact test; the mean lengths of axons sampled between the two groups did not differ, $p=0.97$ mean of 131 μm in each population; Figure 2B). The number of filopodia and branches per 10 μm of axon was also greater in drebrin expressing neurons (Figure 2C, D).

The complex morphology of DRG axons expressing drebrin E1 was also observed *in vitro*. Dissociated E7 chicken sensory neurons were transfected with either RFP-drebrin E1 or RFP alone as a control and cultured for 24 hours (Fig. 3A). Overexpression of RFP-drebrin E1 relative to RFP alone increased the average number of axonal filopodia along the distal 50 μm of the axon, excluding the growth cone (i.e., microns 10–60 from the leading edge of

the growth cone), by 152% (Figure 3B) and the mean number of collateral branches along the same length of axon by 335% (Figure 3C). Overexpression of RFP-drebrin E1 slightly decreased the length of filopodia relative to RFP expressing controls ($p<0.05$, 8.3/5.6 ± 0.8 vs 9.5/7.6 ± 0.7 (mean/median ± SEM), respectively).

Conversely, knockdown of drebrin had a negative effect on axonal filopodia and axonal branching. Embryonic day 7 chicken sensory neurons were transfected with a vector expressing either drebrin shRNA or scrambled shRNA and a GFP-transfection reporter (as characterized in Dun et al., 2012), and cultured *in vitro* for 3 days (Figure 3D–F), a period during which the complexity of axon branching increases relative to 24 hrs of culturing. Consistent with the initial characterization of the efficacy of the shRNA vector in chicken neurons (Dun et al., 2012), immnocytochemical staining for drebrin revealed that the majority of GFP-positive neurons exhibited barely detectable levels of drebrin relative to GFP-positive neurons transfected with scrambled shRNA (Figure 3D), or non-transfected neurons in the same culture (Figure S1). Expression of drebrin shRNA relative to scrambled shRNA decreased the number of axonal filopodia by 69% (Figure 3E–G) and the number of collateral branches in the distal 100 μm of the axon by 53% (Figure 3E,F,H). Depletion of drebrin also greatly decreased the length of filopodia that formed (6.2/5.5 ± 0.3 vs 1.9/1 ± 0.2 (mean/median ± SEM) scrambled and drebrin shRNA respectively; Mann-Whitney test $p<0.0001$). Collectively these data indicate that drebrin positively regulates the number of axonal filopodia and collateral branches along the axons of embryonic chicken sensory neurons.

Drebrin localizes to axonal actin patches and promotes the formation of axonal filopodia by increasing the rate of transition of an actin patch into a filopodium

The emergence of axonal filopodia is the first step in establishing collateral branches, and axonal filopodia arise from transient localized accumulations of actin filaments termed axonal patches. Although axonal filopodia emerge from actin patches, only a subset of actin patches give rise to filopodia prior to dissipating (Loudon et al., 2006; Ketschek and Gallo, 2010). As imaged using fluorescently tagged β-actin, the life cycle of actin patches can be classified into four phases (Figure 4A): (1) the “initiation phase”- the formation of a patch, (2) the “elaboration phase”- the increase in size and actin content of the patch with time, (3) the “dissipation phase”- the shrinkage and fading of a patch, and (4) the “transition phase”- which denotes the emergence of the filopodium from the patch (Loudon et al., 2006). The filopodia often exhibit longer durations than the patches, and the patches dissipate from the base of long lived filopodia.

Endogenous drebrin localized to actin patches (Figure 4B), as determined by immunocytochemistry. To elucidate the mechanism by which drebrin positively regulates the number of axonal filopodia, we first investigated the effects of drebrin on axonal actin patch dynamics and the emergence of filopodia. E7 chicken sensory neurons were transfected with RFP-drebrin E1 and eYFP-β-actin. Consistent with the immunocytochemistry revealing drebrin localizes to axonal actin patches, dual channel live image analysis revealed that accumulations of RFP-drebrin E1 co-localized and formed in synchrony with axonal actin patches (Figure 4C). The average number of new patches formed along a fixed length of

axon per unit time was not altered in neurons expressing RFP-drebrin E1 compared to RFP-controls (11 ± 1.4 vs 12 ± 1.8 patches/40 μm distal axon/5 min (mean ± SEM) respectively; p = 0.6073, Welch t-test; n=15 axons per group as in rest of analysis). There was also no significant difference in the duration of actin patches, the time when the patch is first detectable to when it dissipates back to background levels, between neurons expressing RFP-drebrin E1 compared to RFP-control (42.5/30 ± 3.4 vs 37.4/30 ± 3.2 sec (mean/median ± SEM) respectively, p = 0.29, Mann-Whitney test). However, over-expression of drebrin had a pronounced effect on the frequency at which actin patches transitioned into filopodia. The percentage of patches transitioning into filopodia was increased by 69% in neurons expressing RFP-drebrin E1 compared to RFP-control (29% vs 49% of patches transitioning, respectively; p = 0.0057, Fisher's Exact test).

The axons of sensory neurons transfected with drebrin shRNA, and co-transfected with mCherry-β-actin, to track actin patch dynamics, were imaged three days following plating, when drebrin levels have been knocked down (as in Figure 3). The axons of neurons expressing drebrin shRNA showed a 69% decrease in the percentage of patches that transitioned into filopodia compared to the control scrambled shRNA (11% vs 35% respectively, p = 0.0078, Fisher's Exact test; n=179 and 112 patches for control and drebrin shRNAs sampled from 8 and 17 axons respectively). Analysis of the rate of actin patch formation along the distal 40 μm of axons, as described above, revealed that axons depleted of drebrin generated 70% less actin patches than control neurons (22.3/19.5±3.5 and 6.6/4±1.9, mean/median ± SEM patches/40 μm distal axon/5 min, n=8 and 17 axons for control and drebrin shRNA respectively; p<0.002, Mann-Whitney test;). However, the duration of actin patches that formed along the axons of drebrin depleted neurons exhibited a 52% increase in duration (p<0.001, Mann-Whitney test). Together, the data reveal that endogenous drebrin plays a role in the formation of axonal filopodia by regulating the emergence of filopodia from actin patches. Furthermore, endogenous drebrin contributes to the maintenance of normal levels of actin patch formation and duration, however there was no effect seen on these aspects of patches when drebrin was overexpressed.

Drebrin localizes to the proximal portion of filopodia and promotes the stability of axonal filopodia

Filopodia are dynamic protrusions with bouts of tip extension and retraction. In order for a filopodium to mature into a collateral branch, the filopodium must be stabilized to prevent retraction (Dent et al., 1999; Gallo and Letourneau, 1999; Dent and Kalil, 2001; Spillane et al., 2013). Immunocytochemistry for endogenous drebrin and actin filaments revealed that drebrin partially localized to the proximal shaft of filopodia (<50% of filopodial length) and did not extend distally (Figure 4B, D; red arrowheads in panel D), in 61% of filopodia (n=171, 17 axons). In the remaining 39% of filopodia, drebrin was found throughout the filopodium (Figure 4D, white arrowheads). Similar drebrin distributions have been reported in dendritic filopodia prior to maturation into spines (Takahashi et al., 2003). The filopodia that exhibited drebrin throughout their shaft were on average 4.3±0.3 μm (mean ± SEM) in length, in contrast to 12.8±0.9 μm for those exhibiting only proximal localization of drebrin (p<0.0001). The length of the proximal segment of the filopodium containing drebrin, in filopodia exhibiting partial coverage by drebrin, was 5.5±0.5 μm. When comparing only the

portions of filopodia that contained drebrin, we found no difference ($p>0.05$) between the length of the segments exhibiting drebrin (4.3±0.3 μm vs. 5.5±0.5 μm (mean ± SEM) drebrin throughout filopodia and drebrin in proximal segment of filopodia, respectively). These data indicate that drebrin localizes to approximately the first 5 μm of filopodia, and when filopodia extend further, drebrin remains restricted in the proximal segment of the filopodia. Consideration of the dynamics and lengths attained by filopodia formed in drebrin depleted neurons (using shRNA as in Figure 3) revealed that when filopodia formed, they attained lengths on average 62% shorter than controls. Filopodia that emerged from patches attained maximal lengths of 6.8 ± 0.9 μm and 2.6 ± 0.4 μm for control and drebrin shRNA expressing neurons, respectively ($p<0.002$, mean ± SEM, Welch t-test). In drebrin depleted axons, "filopodial buds" emerged from actin patches but failed to exhibit continued elongation and were resorbed into the axon (Figure 4E).

The observation that drebrin localizes to the proximal filopodial shaft and filopodia exhibited a failure to elongate beyond a few microns along axons depleted of drebrin suggested that drebrin may be involved in the stabilization of the emergent filopodium. To further determine if drebrin plays a role in the stability of axonal filopodia, we performed live-image analysis on E7 DRG neurons transfected with either RFP-drebrin E1 or RFP-control. Through analysis of phase contrast videos of axonal dynamics, we found that newly formed filopodia along the distal axons of neurons expressing drebrin E1 showed 34% longer mean lifespans compared to axonal filopodia of control neurons (Figure 4F; 267.59/300 ± 8.3 vs 199.02/260 ± 11.8 seconds (mean/median ± SEM) n=83 and 92, respectively; $p < 0.0001$, Mann-Whitney test). Additionally, live-imaging analysis revealed that neurons expressing drebrin E1 showed a 50% decrease in the number of axonal filopodia exhibiting dynamic tips, characterized by bouts of elongation and retraction, compared to control neurons (40% vs 82% respectively, $p<0.0001$, Fisher's Exact Test). Furthermore, 10% and 40% of axonal filopodia in drebrin E1 and RFP expressing neurons fully retracted back into the axon shaft during the imaging periods ($p<0.0001$, Fischer's exact test). Finally, the over-expressed RFP-drebrin E1 was found localized throughout filopodia (Figure 4G) in 94% of filopodia (n=208), consistent with observed effects on the stability of filopodia at a distance along the filopodial shaft at which endogenous drebrin is not usually found (Figure 4B, D).

We also considered the distribution of endogenous drebrin along the shafts of branches at different stages of maturation. Nascent branches less than 15 μm in length which had begun to attain polarity (i.e., actin filaments redistributed distally and exhibiting additional laterally projecting filopodia) exhibited drebrin along their shaft, but filopodia emerging from the sides of the branch, similar to the axon, only exhibited proximal targeting of drebrin (Figure 4H). Matured branches, with clearly distally polarized actin filaments and additional protrusive structures from their shafts, similarly exhibited drebrin throughout the shaft and drebrin was restricted to the proximal portions of filopodia (Figure 4H).

Drebrin promotes the entry of microtubule tips into axonal filopodia

Microtubules are required for the maturation of filopodia into axonal branches (Gallo, 2011), but the mechanisms through which microtubules become targeted to axonal filopodia are not

well understood. EB3 is a microtubule plus tip tracking protein that is used to report on the dynamics of actively polymerizing microtubules (Stepanova et al., 2003). In live imaging protocols, GFP-EB3 expressed in cells, gives rise to “comet” like signals which report on the dynamics of individual microtubule plus tips (Stepanova et al., 2003), as we have also previously reported for chicken sensory axons (Jones et al., 2006; Ketschek et al., 2007; Spillane et al., 2012). To determine if drebrin regulates the targeting of microtubules into axonal filopodia, we monitored the entry of EB3-comets in axonal filopodia of neurons transfected with both RFP-drebrin E1 and GFP-EB3 relative to RFP-control and GFP-EB3. Live imaging analysis revealed that expression of RFP-drebrin E1 did not change the number of EB3 comets detected per unit length/time in axons ($p>0.05$), indicating that drebrin does not regulate the initiation of microtubule plus tip polymerization in axons. However, expression of RFP-drebrin E1 significantly increased the percentage of axonal filopodia that were invaded by one or more EB3 comets (Figure 5A), compared to the RFP control. During the imaging period (5 min), only 3% of axonal filopodia in RFP-control neurons were invaded by an EB3 comet compared to 24% of axonal filopodia in neurons expressing RFP-drebrin E1 ($p = 0.0001$, Fisher’s Exact test). Additionally, expression of drebrin E1 increased instances of multiple invasions (>1) by EB3 comets of the same filopodium ($p=0.02$; $n=91$ and 80 filopodia for RFP-control and RFP-drebrin E1, respectively). We did not observe an effect of drebrin expression on the distance that microtubule tips penetrated into filopodia relative to controls ($p=0.7$, Mann-Whitney test). These data indicate that drebrin promotes the initial entry of microtubule tips into axonal filopodia, but not the extent of their penetration within the shaft.

The promotion of microtubule targeting to axonal filopodia does not contribute to the stabilization of axonal filopodia by drebrin over-expression

The targeting of microtubules into filopodia could result in the stabilization of filopodia through either active signaling or mechanical/structural mechanisms. To address whether the increase in microtubule targeting into filopodia observed with drebrin over-expression contributes to the correlated increase in stability of the filopodia, we used vinblastine to attenuate microtubule plus end dynamics in neurons (Baas and Ahmad, 1993; Gallo, 1998; Gallo and Letourneau, 1999). In preliminary work (data not shown), through dose-dependency analysis we determined that in the current culturing conditions a 30 min treatment with 3 nM vinblastine decreased the entry of GFP-EB3 comets into axonal filopodia by 92% and 90% in control RFP and RFP-drebrin E1 expressing axons, respectively, without affecting net levels of microtubules in axons. Treatment with 3 nM vinblastine for 30 min did not affect the lifespan of filopodia in either control RFP or RFP-drebrin E1 expressing neurons (Figure 5B), relative to pre-treatment in the same set of neurons. Vinblastine treatment also did not affect the percentage of filopodia that exhibited dynamics in either RFP or RFP-drebrin E1 expression conditions ($p>0.05$ for comparison in both conditions). These data indicate that the targeting of microtubules to axonal filopodia does not regulate their dynamics and that the effects of drebrin expression on the stabilization of filopodia are independent of its effects promoting the targeting of microtubules into filopodia.

Myosin II inhibition further increases branching along the axons of drebrin over-expressing neurons

Drebrin can regulate the extension of cultured central nervous system axons through a myosin II-dependent mechanism (Mizui et al., 2009) and drebrin binding to actin filaments can inhibit actomyosin contractility by reducing the sliding velocity of actin filaments on substratum-bound myosin and inhibiting the filament-binding associated activation of myosin II ATPase activity (Hayashi et al., 1996). Thus, the effects of drebrin E1 overexpression on filopodia and branches may be due in part to impairment of actomyosin function, which negatively regulates both the formation of filopodia and branches (Loudon et al., 2006; Ketschek at al., 2015). In order to gain insights into possible roles of myosin II in the effects of drebrin overexpression, we analyzed whether treatment with blebbistatin, a pharmacological inhibitor of myosin II activity (Straight et al., 2003), would affect branching in drebrin over-expressing neurons. We found that a 30 min treatment with 50 μM blebbistatin, which is a maximally effective concentration in this culturing system (Gallo, 2004), further increased branching along the axons of drebrin E1 over-expressing neurons (Figure 6A). Drebrin E1 over-expressing axons treated with DMSO or blebbistatin exhibited 1.1/1±0.2 (n=40) and 2.6/3±0.3 (n=35) branches along their distal axons, respectively (mean/median + SEM; $p<0.0001$, Mann-Whitney test). Blebbistatin treatment also increased the length of axon branches from 33/27±2.2 (n=61; DMSO) to 48/56±2.0 μm (n=94; blebbistatin) (mean/median ± SEM; $p<0.0001$, Mann-Whitney test). Analysis of the rate of filopodia formation did not reveal an increase after blebbistatin treatment in drebrin E1 over-expressing axons (0.7/0±0.2 and 0.6/0±0.2 filopodia/40 μm axon pre and post treatment respectively, n=19 axons; mean/median + SEM; $p=0.46$ Wilcoxon matched pairs test). Blebbistatin treatment also did not affect the length of filopodia (8.2/6.9±0.5 and 8.4/6.7±0.5 μm pre (n=155) and post (n=139) treatment respectively; mean/median + SEM; $p=0.9$ Wilcoxon matched pairs test).

Myosin II directly controls the actin cytoskeleton and indirectly affects the ability of microtubules to penetrate cellular domains enriched in actin through the regulation of the retrograde flow of actin filaments (Schaefer et al, 2008). In embryonic sensory axons, inhibition of myosin II increases the distance that microtubule tips penetrate into axonal filopodia both along the axon and at the growth cone (Ketschek et al., 2007, 2015). To gain insights into the effects of blebbistatin on the axons of drebrin over-expressing neurons, we imaged the dynamics of microtubule plus tips in drebrin E1 over-expressing neurons pre and post treatment with 50μM blebbistatin (n=10 axons). Blebbistatin treatment did not affect the percentage of filopodia that were invaded by EB3 comets (12% (97 filopodia) and 14% (95 filopodia), $p=0.85$, for pre and post treatment). Blebbistatin treatment increased the distance that microtubule tips penetrated into the shafts of filopodia by 34% (58/59 ± 7% and 78/83 ± 6% of filopodia shaft penetration pre and post treatment, n=12 and 14 filopodia; mean/median + SEM; $p=0.05$ Wilcoxon matched pairs test) and in the same set of filopodia did not affect filopodial length ($p=0.63$), as also described above.

Inhibition of myosin II activity promotes the localization of endogenous drebrin to the distal part of axonal filopodia

Inhibition of myosin II using blebbistatin promotes the branching of axons (Ketschek et al., 2015). We thus sought to determine if inhibition of myosin II affects the distribution of drebrin along axonal filopodia. Treatment of neurons cultured overnight in the presence of NGF with blebbistatin for 30 min resulted in increased targeting of endogenous drebrin along the distal shaft of filopodia (Figure 6B,C). In control samples treated with DMSO drebrin localized along the proximal 50/45 ± 0.3% of the filopodial shaft (mean/median ±SEM; n=106 filopodia). In blebbistatin treated samples drebrin was detected along 89/100 ± 1.8% of the filopodial shaft (n=101 filopodia; $p<0.0001$ relative to DMSO). These data indicate that the proximo-distal localization of endogenous drebrin within axonal filopodia is negatively regulated by myosin II activity.

Inhibition of myosin II increases the distance that microtubules penetrate into axonal filopodia (Ketschek et al., 2015) and drebrin can associate with EB3 on the tips of microtubules (Geraldo et al., 2008). We therefore sought to determine if the promotion of microtubule penetration into filopodia may underlie the observed distal targeting of drebrin within filopodia following inhibition of myosin II. Cultures were pretreated with 3 nM VB, as in the prior experiments, and then with blebbistatin. Treatment with VB to attenuate microtubule tip targeting into filopodia did not alter the blebbistatin induced redistribution of drebrin into the distal compartment of axonal filopodia (Figure 6B,C).

Given that prior data implicate drebrin in the stabilization of filopodia, we sought to determine if the redistribution of drebrin into distal filopodia induced by blebbistatin correlated with increased filopodial stability. Consideration of the percentage of axonal filopodia that exhibited tip dynamics (cycles of protrusion or retraction) before and after treatment with blebbistatin showed a mild but significant 17% decrease in the percentage of dynamic filopodia/axon after blebbistatin ($p<0.03$, paired t-test, n=11 axons). Similarly, consideration of the lifespans of filopodia also revealed that post-blebbistatin treatment lifespans were increased by 12% ($p<0.0001$, Wilcoxon matched-pairs signed-ranks test, n=168 and 137 filopodia). These data are consistent with the notion that the blebbistatin induced redistribution of drebrin into filopodia may contribute to increased filopodia stability, but as myosin II has multiple roles in the regulation of filopodia and the cytoskeleton may also be reflective of non-drebrin related effects.

NGF increases the protein levels of drebrin in axons

The induction of filopodia and collateral branches along embryonic sensory axons by NGF is dependent on the intra-axonal synthesis of cytoskeletal proteins that regulate the Arp2/3 cytoskeleton (Spillane et al., 2012). Axonal mRNA coding for drebrin has been reported in embryonic but not adult sensory axons (Gumy et al., 2011). Therefore, we sought to determine if NGF regulates the axonal levels of drebrin in a manner sensitive to the translational inhibitor cycloheximide, a test of whether drebrin may be locally synthesized. As in Spillane et al (2012), we cultured E7 sensory explants overnight in no NGF, and just prior to the addition of NGF (40 ng/mL), the axons extending from the explants were severed from the cell bodies at the point of their emergence from the explants to prevent

contributions from the cell bodies. Control axons were similarly severed but treated with NGF storage buffer. Cultures were then fixed 30 min after treatment with NGF or control buffer and stained with antibodies to drebrin. Quantification of the total intensity of drebrin staining along the distal 50 μm of axons revealed that NGF treatment increased the levels of drebrin relative to controls (Figure 7). Pretreatment of the cultures with the translational inhibitor cycloheximide (35 μM, 15 min pretreatment) followed by treatment with NGF did not affect the NGF-induced increases in the levels of drebrin within distal axons (Figure 7A,B). Treatment with cycloheximide alone did not affect the baseline levels of drebrin in the absence of NGF treatment (Figure 7A,B). As a positive control for the effects of cycloheximide we measured the levels of axonal actin filaments, which are increased by NGF treatment in a protein synthesis dependent manner (Spillane et al., 2012), and found that cycloheximide inhibited the effect of NGF in the same population of axons in which the levels of drebrin were measured (not shown). We also determined the effects of an additional inhibitor of protein synthesis on the NGF-induced increase in the axonal levels of drebrin, anisomycin (40 μM). Anisomycin pretreatment did not affect the NGF-induced increase in drebrin levels (Figure 7C). As a positive control, we determined the effects of anisomycin on the NGF-induced increase in axonal levels of cortactin, an actin regulatory protein which is locally synthesized in axons in response to NGF (Spillane et al., 2012). In contrast to drebrin, anisomycin blocked the NGF-induced increase in cortactin levels (Figure 7C; see Figure S2 for examples of cortactin staining levels in axons). Thus, these data reveal that NGF increases the levels of drebrin in distal axons, but do not support the notion that NGF drives the intra-axonal synthesis of drebrin.

DISCUSSION

The formation of axon collateral branches is dependent on complex interactions between actin filaments and microtubules (Dent and Kalil, 2001; Gallo, 2011; Kalil and Dent, 2014). The current investigation sought to elucidate the role of drebrin in the cytoskeletal events underlying the formation of sensory axon collateral branches. The data reveal that drebrin positively regulates the formation of branches through the promotion of the formation of axonal filopodia from their precursor structures (actin patches) and the targeting of microtubules into filopodia. Collectively, the data indicate that drebrin coordinates the actin filament and microtubule cytoskeleton during the initial stages of axon branching. The main conclusions suggested by this study are summarized in Figure 8.

Endogenous drebrin localizes to actin patches and extends approximately 4–5 μm into axonal filopodia. This localization is consistent with its roles in promoting the emergence of filopodia from actin patches and the targeting of microtubules into filopodia. The emergence of filopodia from actin patches is considered to occur through an actin filament network convergence mechanism (Spillane et al., 2011; Svitkina, 2013). In this mechanism, actin filaments are nucleated into meshworks by the activity of the actin nucleating factor Arp2/3, and a subpopulation of the filaments are subsequently bundled giving rise to the emergent filopodial shaft. The observation that when drebrin is depleted “filopodial-buds” appeared to initiate from actin patches, but fail to subsequently elongate beyond a few of microns, indicates that drebrin may be involved in the initial bundling of filaments within actin patches as the filopodium begins to emerge. Consistent with this notion, drebrin exhibits

actin filament bundling activity which is promoted by phosphorylation by cyclin dependent kinase 5 (Cdk5) (Worth et al., 2013). Fascin is an additional actin filament bundling protein that is considered to contribute to the bundling of filaments during filopodia elongation in the network convergence mechanism and targets the entire length of filopodia (Vignjevic et al., 2006). Interestingly, purified drebrin impairs fascin mediated actin filament bundling in vitro (Sasaki et al., 1996). Thus, drebrin may be involved in the initial stages of the bundling of actin filaments during the emergence of filopodia and fascin may in turn control bundling in the more distal shaft of the filopodia.

The data indicate that drebrin is involved in the stabilization of filopodia, and stabilization is also likely to contribute to the failure of filopodia to extend under conditions of drebrin depletion. Drebin can stabilize actin filaments by inhibiting depolymerization of the barbed ends (Mikati et al., 2013). Cofilin and actin depolymerizing factor are proteins that promote actin filament severing and the depolymerization of filaments (Bravo-Cordero et al., 2013). Drebrin binding to filaments can compete with cofilin and impair its ability to sever filaments (Grintsevich and Reisler, 2014). Spikar is a drebrin binding protein shown to be required for dendritic spine maintenance. Depletion of spikar results in increased retraction of spines (Yamazaki et al., 2014) indicating decreased stability of the underlying cytoskeleton. Whether spikar is found in axonal filopodia remains to be determined.

Even though the current study is consistent with the notion that drebrin has a role in filament stabilization within filopodia and filopodia stability, surprisingly the few actin patches that formed when drebrin was depleted using shRNA exhibited a greater duration suggesting increased stability of filaments in patches. This discrepancy may reflect differences in the cohort of proteins active in patches relative to filopodia, differences in filament organization (meshworks in patches and bundles in filopodia) and the complex effects of drebrin on multiple actin binding proteins (Dun and Chilton, 2010). The shRNA depletion results indicate that endogenous drebrin contributes to the formation of actin patches. However, overexpression of drebrin did not further increase the rate of formation of actin patches or duration of patches, indicating a required but not sufficient role for drebrin in patch formation.

The initiation of sensory axon branching in response to NGF requires NGF-induced intra-axonal protein synthesis of actin regulators (Spillane et al., 2012). Drebrin mRNA has been reported to target embryonic sensory axons (Gumy et al., 2011). We find that NGF increases axonal levels of drebrin in embryonic sensory neurons within 30 min of treatment in a cycloheximide and anisomycin insensitive manner. The data thus do not support the notion that NGF regulates the axonal levels of drebrin through localized protein synthesis. Interestingly, NGF promotes the targeting of microtubules into axonal filopodia in a manner independent of intra-axonal protein synthesis (Spillane et al., 2012). The observations that drebrin promotes microtubule targeting into filopodia, and NGF regulates drebrin levels independent of protein synthesis, is thus consistent with a protein synthesis-independent aspect of the NGF-regulated branching mechanism that controls microtubule based events during branching (Spillane et al, 2012).

Two not mutually exclusive additional possibilities can be considered for the observed increase in drebrin levels; (1) NGF may increase the axonal transport of drebrin into distal axons, and (2) NGF may decrease drebrin degradation. The mechanism of the axonal transport of drebrin is not known, nor is it known whether it is conveyed by fast or slow transport. Additional studies will need to address the transport of drebrin and whether it may be under regulation by NGF. Similarly, the mechanism controlling the turnover of drebrin is not known. However, in the context of neurotrophin-induced increases in the levels of axonal cortactin, both intra-axonal synthesis and the inhibition of calpain mediated proteolysis have been considered (Mingorance-Le Meur and O'Connor, 2009; Spillane et al., 2012). Interestingly, drebrin is degraded through calpain-mediated proteolysis in neurotoxic models (Chimura et al., 2015) and NGF decreases calpain activity in PC12 cells (Oshima et al., 1989; Pintér a., 1994). Thus, in future work, it will be of interest to determine if NGF may control drebrin levels through the negative regulation of drebrin degradation/proteolysis.

Cdk5 has been shown to phosphorylate drebrin and promote its filament bundling activity (Worth et al., 2013). NGF has been shown to positively regulate Cdk5 activity (Li et al., 2007; Chen et al., 2010), and may thus also control drebrin through a phosphorylation based mechanism. Phosphatase and tensin homolog (PTEN) is generally considered to be a lipid phosphosphatase that antagonizes the activation of the Akt-mTOR pathway by phosphoinositide 3-kinase activity (van Diepen and Eickholt, 2008; Kreis et al., 2014). However, PTEN also has phosphatase activity toward some proteins and PTEN mediates the dephosphorylation of S647 in the C domain of drebrin (Kreis et al., 2013). Although the full spectrum of the role of S647 phosphorylation is not well understood, it is considered to positively regulate drebrin functions. NGF induced axon branching is mediated by activation of PI3K (Ketschek and Gallo, 2010; Spillane et al., 2012) and PTEN negatively regulates axon branching (Kwon et al., 2006). While NGF is well established to activate PI3K signaling (Huang and Reichardt, 2003; Zhou and Snider, 2006), it is not known whether NGF may act through the impairment of PTEN activity, but it will be of interest to further detail the role of PTEN and drebrin in the effects of NGF.

The current study reveals that drebrin promotes the entry of microtubule plus tips into axonal filopodia, a fundamental and required aspect of the mechanism of axon branching. The promotion of microtubule targeting by drebrin has also been observed in dendritic spines (Merriam et al., 2013), indicating a conservation of function between axonal and dendritic protrusions. Septin 7 has also been reported to promote the targeting of microtubules into axonal filopodia during axon branching (Hu et al., 2012). Interestingly, unlike drebrin which localizes up to approximately 5 μm into filopodia, septin 7 targets specifically at the base of axonal filopodia and does not extend further. Thus, septin 7 and drebrin may cooperate in the initial capture of microtubule tips and delivery into the most proximal part of the filopodium, and drebrin may then continue to guide the microtubule tip further into the filopodial shaft beyond the base where the initial capture of the microtubule tip from the axon shaft is considered to occur.

Myosin II negatively regulates axon branching and further promotes NGF-induced branching (Ketschek et al., 2015). Along axons, myosin II serves to suppress formation of filopodia and also decreases the distance microtubules penetrate into filopodia but does not

increase the targeting of microtubules into filopodia (Ketschek et al., 2015). Drebrin interacting with myosin II can impair actomyosin contractility (Hayashi et al., 1996) leading us to consider whether the increase in branching observed following drebrin over-expression may be due to the inhibition of actomyosin along the axons. The observation that inhibition of myosin II using blebbistatin further increased branching along axons over-expressing drebrin-E1 indicates that the effects seen under these conditions are not due to maximal suppression of actomyosin contractility by drebrin. Blebbistatin treatment promoted the penetration of microtubules into filopodia in drebrin overexpressing neurons, indicating that drebrin is not overtly involved in the suppression of this function of myosin II in filopodia. The promotion of microtubule penetration into filopodia in this context may however underlie the observed increase in branching following inhibition of myosin II in drebrin overexpressing neurons. Inhibition of myosin II also promoted the targeting of endogenous drebrin into the distal portions of axonal filopodia, similar to the localization of overexpressed drebrin. Interestingly, both inhibition of myosin II (Ketschek et al., 2015) and overexpression of drebrin independently promote branching. These observations suggest that the redistribution of drebrin into the distal filopodium may represent a component of the mechanism which promotes branching when myosin II is inhibited. Inhibition of myosin II increases the distance that microtubule tips penetrate into filopodia (Ketschek et al., 2015), an effect which may be facilitated or orchestrated by the presence of drebrin in the distal portion of filopodia, thereby promoting branching by allowing drebrin to guide microtubule plus tips towards the tip of the filopodium.

Supplementary Material

Refer to Web version on PubMed Central for supplementary material.

Acknowledgments

This work was supported by an NIH award to GG (NS078030) and Wellcome Trust (080045/Z/06/Z) and BBSRC (BB/I001255/1) project grants to JC

Referenced Literature

Baas PW, Ahmad FJ. The transport properties of axonal microtubules establish their polarity orientation. J Cell Biol. 1993; 120:1427–37. [PubMed: 8449987]

Bazellières E, Massey-Harroche D, Barthélémy-Requin M, Richard F, Arsanto JP, Le Bivic A. Apico-basal elongation requires a drebrin-E-EB3 complex in columnar human epithelial cells. J Cell Sci. 2012; 125:919–31. [PubMed: 22275434]

Bravo-Cordero JJ, Magalhaes MA, Eddy RJ, Hodgson L, Condeelis J. Functions of cofilin in cell locomotion and invasion. Nat Rev Mol Cell Biol. 2013; 14:405–15. [PubMed: 23778968]

Chen MC, Lin H, Hsu FN, Huang PH, Lee GS, Wang PS. Involvement of cAMP in nerve growth factor-triggered p35/Cdk5 activation and differentiation in PC12 cells. Am J Physiol Cell Physiol. 2010; 299:C516–27. [PubMed: 20463173]

Chimura T, Launey T, Yoshida N. Calpain-Mediated Degradation of Drebrin by Excitotoxicity In vitro and In vivo. PLoS One. 2015; 10(4):e0125119. [PubMed: 25905636]

Dent EW, Callaway JL, Szebenyi G, Baas PW, Kalil K. Reorganization and movement of microtubules in axonal growth cones and developing interstitial branches. J Neurosci. 1999; 19:8894–908. [PubMed: 10516309]

Dent EW, Kalil K. Axon branching requires interactions between dynamic microtubules and actin filaments. J Neurosci. 2001; 21:9757–69. [PubMed: 11739584]

Dent EW, Gertler FB. Cytoskeletal dynamics and transport in growth cone motility and axon guidance. Neuron. 2003; 40:209–27. [PubMed: 14556705]

Dun XP, Chilton JK. Control of cell shape and plasticity during development and disease by the actin-binding protein Drebrin. Histol Histopathol. 2010; 25:533–40. [PubMed: 20183806]

Dun XP, Bandeira de Lima T, Allen J, Geraldo S, Gordon-Weeks P, Chilton JK. Drebrin controls neuronal migration through the formation and alignment of the leading process. Mol Cell Neurosci. 2012; 49:341–50. [PubMed: 22306864]

Fukushima N, Furuta D, Tsujiuchi T. Coordinated interactions between actin and microtubules through crosslinkers in neurite retraction induced by lysophosphatidic acid. Neurochem Int. 2011; 59:109–13. [PubMed: 21693153]

Gallo G. Involvement of microtubules in the regulation of neuronal growth cone morphologic remodeling. J Neurobiol. 1998; 35:121–40. [PubMed: 9581969]

Gallo G. Myosin II activity is required for severing-induced axon retraction in vitro. Exp Neurol. 2004; 189:112–21. [PubMed: 15296841]

Gallo G. The cytoskeletal and signaling mechanisms of axon collateral branching. Dev Neurobiol. 2011; 71:201–20. [PubMed: 21308993]

Gallo G. Mechanisms underlying the initiation and dynamics of neuronal filopodia: from neurite formation to synaptogenesis. Int Rev Cell Mol Biol. 2013; 301:95–156. [PubMed: 23317818]

Gallo G, Letourneau PC. Localized sources of neurotrophins initiate axon collateral sprouting. J Neurosci. 1998; 18:5403–14. [PubMed: 9651222]

Gallo G, Letourneau PC. Different contributions of microtubule dynamics and transport to the growth of axons and collateral sprouts. J Neurosci. 1999; 19:3860–73. [PubMed: 10234018]

Geraldo S, Khanzada UK, Parsons M, Chilton JK, Gordon-Weeks PR. Targeting of the F-actin-binding protein drebrin by the microtubule plus-tip protein EB3 is required for neuritogenesis. Nat Cell Biol. 2008; 10:1181–9. [PubMed: 18806788]

Gibson DA, Ma L. Developmental regulation of axon branching in the vertebrate nervous system. Development. 2011; 138:183–95. [PubMed: 21177340]

Goryunov D, He CZ, Lin CS, Leung CL, Liem RK. Nervous-tissue-specific elimination of microtubule-actin crosslinking factor 1a results in multiple developmental defects in the mouse brain. Mol Cell Neurosci. 2010; 44:1–14. [PubMed: 20170731]

Grintsevich EE, Reisler E. Drebrin inhibits cofilin-induced severing of F-actin. Cytoskeleton. 2014; 71:472–83. [PubMed: 25047716]

Gumy LF, Yeo GS, Tung YC, Zivraj KH, Willis D, Coppola G, Lam BY, Twiss JL, Holt CE, Fawcett JW. Transcriptome analysis of embryonic and adult sensory axons reveals changes in mRNA repertoire localization. RNA. 2011; 17:85–98. [PubMed: 21098654]

Hayashi K, Ishikawa R, Ye LH, He XL, Takata K, Kohama K, Shirao T. Modulatory role of drebrin on the cytoskeleton within dendritic spines in the rat cerebral cortex. J Neurosci. 1996; 16:7161–70. [PubMed: 8929425]

Houseweart MK, Cleveland DW. Cytoskeletal linkers: new MAPs for old destinations. Curr Biol. 1999; 9:R864–6. [PubMed: 10574751]

Hu J, Bai X, Bowen JR, Dolat L, Korobova F, Yu W, Baas PW, Svitkina T, Gallo G, Spiliotis ET. Septin-driven coordination of actin and microtubule remodeling regulates the collateral branching of axons. Curr Biol. 2012; 22:1109–15. [PubMed: 22608511]

Huang EJ, Reichardt LF. Trk receptors: roles in neuronal signal transduction. Annu Rev Biochem. 2003; 72:609–42. [PubMed: 12676795]

Huber P, Bouillot S, Elsen S, Attrée I. Sequential inactivation of Rho GTPases and Lim kinase by Pseudomonas aeruginosa toxins ExoS and ExoT leads to endothelial monolayer breakdown. Cell Mol Life Sci. 2014; 71:1927–41. [PubMed: 23974244]

Jones SL, Selzer ME, Gallo G. Developmental regulation of sensory axon regeneration in the absence of growth cones. J Neurobiol. 2006; 66:1630–45. [PubMed: 17058187]

Kalil K, Dent EW. Branch management: mechanisms of axon branching in the developing vertebrate CNS. Nat Rev Neurosci. 2014; 15:7–18. [PubMed: 24356070]

Ketschek AR, Jones SL, Gallo G. Axon extension in the fast and slow lanes: substratum-dependent engagement of myosin II functions. Dev Neurobiol. 2007; 67:1305–20. [PubMed: 17638383]

Ketschek A, Gallo G. Nerve growth factor induces axonal filopodia through localized microdomains of phosphoinositide 3-kinase activity that drive the formation of cytoskeletal precursors to filopodia. J Neurosci. 2010; 30:12185–97. [PubMed: 20826681]

Ketschek A, Jones S, Spillane M, Korobova F, Svitkina T, Gallo G. Nerve growth factor promotes reorganization of the axonal microtubule array at sites of axon collateral branching. Dev Neurobiol. 2015; In press. doi: 10.1002/dneu.22294

Kojima N, Shirao T, Obata K. Molecular cloning of a developmentally regulated brain protein, chicken drebrin A and its expression by alternative splicing of the drebrin gene. Brain Res Mol Brain Res. 1993; 19(1–2):101–14. [PubMed: 8361332]

Kreis P, Hendricusdottir R, Kay L, Papageorgiou IE, van Diepen M, Mack T, Ryves J, Harwood A, Leslie NR, Kann O, Parsons M, Eickholt BJ. Phosphorylation of the actin binding protein Drebrin at S647 is regulated by neuronal activity and PTEN. PLoS One. 2013; 8:e71957. [PubMed: 23940795]

Kreis P, Leondaritis G, Lieberam I, Eickholt BJ. Subcellular targeting and dynamic regulation of PTEN: implications for neuronal cells and neurological disorders. Front Mol Neurosci. 2014; 7:23. [PubMed: 24744697]

Kwon CH, Luikart BW, Powell CM, Zhou J, Matheny SA, Zhang W, Li Y, Baker SJ, Parada LF. Pten regulates neuronal arborization and social interaction in mice. Neuron. 2006; 50:377–88. [PubMed: 16675393]

Lelkes, PI.; Unsworth, BR.; Saporta, S.; Cameron, DF.; Gallo, G. Culture of Neuroendocrine and Neuronal Cells for Tissue Engineering. In: Vunjak-Novakovic, G.; Freshney, RI., editors. Culture of Cells for Tissue engineering. Vol. Chapter 14. New York: Wiley Inc; 2006.

Li T, Chalifour LE, Paudel HK. Phosphorylation of protein phosphatase 1 by cyclin-dependent protein kinase 5 during nerve growth factor-induced PC12 cell differentiation. J Biol Chem. 2007; 282:6619–28. [PubMed: 17202132]

Loudon RP, Silver LD, Yee HF Jr, Gallo G. RhoA-kinase and myosin II are required for the maintenance of growth cone polarity and guidance by nerve growth factor. J Neurobiol. 2006; 66:847–67. [PubMed: 16673385]

Merriam EB, Millette M, Lumbard DC, Saengsawang W, Fothergill T, Hu X, Ferhat L, Dent EW. Synaptic regulation of microtubule dynamics in dendritic spines by calcium, F-actin, and drebrin. J Neurosci. 2013; 33:16471–82. [PubMed: 24133252]

Mikati MA, Grintsevich EE, Reisler E. Drebrin-induced stabilization of actin filaments. J Biol Chem. 2013; 288:19926–38. [PubMed: 23696644]

Mingorance-Le Meur A, O'Connor TP. Neurite consolidation is an active process requiring constant repression of protrusive activity. EMBO J. 2009; 28:248–60. [PubMed: 19096364]

Mizui T, Kojima N, Yamazaki H, Katayama M, Hanamura K, Shirao T. Drebrin E is involved in the regulation of axonal growth through actin-myosin interactions. J Neurochem. 2009; 109:611–22. [PubMed: 19222710]

Onifer SM, Smith GM, Fouad K. Plasticity after spinal cord injury: relevance to recovery and approaches to facilitate it. Neurotherapeutics. 2011; 8:283–93. [PubMed: 21384221]

Oshima M, Koizumi S, Fujita K, Guroff G. Nerve growth factor-induced decrease in the calpain activity of PC12 cells. J Biol Chem. 1989; 264:20811–6. [PubMed: 2555371]

Pintér M, Aszódi A, Friedrich P, Ginzburg I. Calpeptin, a calpain inhibitor, promotes neurite elongation in differentiating PC12 cells. Neurosci Lett. 1994; 170:91–3. [PubMed: 8041520]

Rodriguez OC, Schaefer AW, Mandato CA, Forscher P, Bement WM, Waterman-Storer CM. Conserved microtubule-actin interactions in cell movement and morphogenesis. Nat Cell Biol. 2003; 5:599–609. [PubMed: 12833063]

Sasaki Y, Hayashi K, Shirao T, Ishikawa R, Kohama K. Inhibition by drebrin of the actin-bundling activity of brain fascin, a protein localized in filopodia of growth cones. J Neurochem. 1996; 66:980–8. [PubMed: 8769857]

Schaefer AW, Schoonderwoert VT, Ji L, Mederios N, Danuser G, Forscher P. Coordination of actin filament and microtubule dynamics during neurite outgrowth. Dev Cell. 2008; 15:146–62. [PubMed: 18606148]

Spillane M, Ketschek A, Jones SL, Korobova F, Marsick B, Lanier L, Svitkina T, Gallo G. The actin nucleating Arp2/3 complex contributes to the formation of axonal filopodia and branches through the regulation of actin patch precursors to filopodia. Dev Neurobiol. 2011; 71:747–58. [PubMed: 21557512]

Spillane M, Ketschek A, Donnelly CJ, Pacheco A, Twiss JL, Gallo G. Nerve growth factor-induced formation of axonal filopodia and collateral branches involves the intra-axonal synthesis of regulators of the actin-nucleating Arp2/3 complex. J Neurosci. 2012; 32:17671–89. [PubMed: 23223289]

Spillane M, Ketschek A, Merianda TT, Twiss JL, Gallo G. Mitochondria coordinate sites of axon branching through localized intra-axonal protein synthesis. Cell Rep. 2013; 5:1564–75. [PubMed: 24332852]

Spillane M, Gallo G. Involvement of Rho-family GTPases in axon branching. Small GTPases. 2014 In Press.

Stepanova T, Slemmer J, Hoogenraad CC, Lansbergen G, Dortland B, De Zeeuw CI, Grosveld F, van Cappellen G, Akhmanova A, Galjart N. Visualization of microtubule growth in cultured neurons via the use of EB3-GFP (end-binding protein 3-green fluorescent protein). J Neurosci. 2003; 23:2655–64. [PubMed: 12684451]

Straight AF, Cheung A, Limouze J, Chen I, Westwood NJ, Sellers JR, Mitchison TJ. Dissecting temporal and spatial control of cytokinesis with a myosin II Inhibitor. Science. 2003; 299:1743–7. [PubMed: 12637748]

Svitkina TM. Ultrastructure of protrusive actin filament arrays. Curr Opin Cell Biol. 2013; 25:574–81. [PubMed: 23639311]

Takahashi H, Sekino Y, Tanaka S, Mizui T, Kishi S, Shirao T. Drebrin-dependent actin clustering in dendritic filopodia governs synaptic targeting of postsynaptic density-95 and dendritic spine morphogenesis. J Neurosci. 2003; 23:6586–95. [PubMed: 12878700]

van Diepen MT, Eickholt BJ. Function of PTEN during the formation and maintenance of neuronal circuits in the brain. Dev Neurosci. 2008; 30:59–64. [PubMed: 18075255]

Vignjevic D, Kojima S, Aratyn Y, Danciu O, Svitkina T, Borisy GG. Role of fascin in filopodial protrusion. J Cell Biol. 2006; 174:863–75. [PubMed: 16966425]

Villarroel-Campos D, Gonzalez-Billault C. The MAP1B case: An old MAP that is new again. Dev Neurobiol. 2014; 74:953–71. [PubMed: 24700609]

Worth DC, Daly CN, Geraldo S, Oozeer F, Gordon-Weeks PR. Drebrin contains a cryptic F-actin-bundling activity regulated by Cdk5 phosphorylation. J Cell Biol. 2013; 202:793–806. [PubMed: 23979715]

Yamazaki H, Kojima N, Kato K, Hirose E, Iwasaki T, Mizui T, Takahashi H, Hanamura K, Roppongi RT, Koibuchi N, Sekino Y, Mori N, Shirao T. Spikar, a novel drebrin-binding protein, regulates the formation and stabilization of dendritic spines. J Neurochem. 2014; 128:507–22. [PubMed: 24117785]

Zhou FQ, Snider WD. Intracellular control of developmental and regenerative axon growth. Philos Trans R Soc Lond B Biol Sci. 2006; 361:1575–92. [PubMed: 16939976]

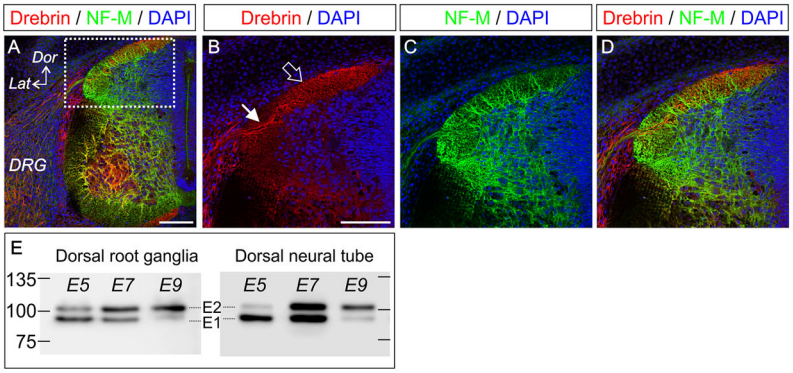

Figure 1.

Drebrin is expressed within the axons of sensory neurons within the spinal cord. **(A)** Antibody labelling of drebrin (red) and neurofilament medium chain (NF-M, green) in transverse sections of E7 spinal cord imaged using confocal microscopy. Cell nuclei are labelled with DAPI (blue). Dorsal (Dor) and lateral (Lat) axis are shown in the panel, as well as the location of the dorsal root ganglion (DRG). **(B–D)** Higher magnification view of the area boxed in (A) showing drebrin expression in axons entering the spinal cord (filled arrow) and in the dorsal column (open arrow). Scale bars = 100 μm. **(E)** Western blots of drebrin expression in lysates of dorsal rooot ganglia and dorsal spinal cord at E5, E7 and E9. The lower band is the drebrin E1 isoform, the upper band is drebrin E2, these undergo developmental regulation of their relative levels of expression. Protein sizes in kDa are indicated.

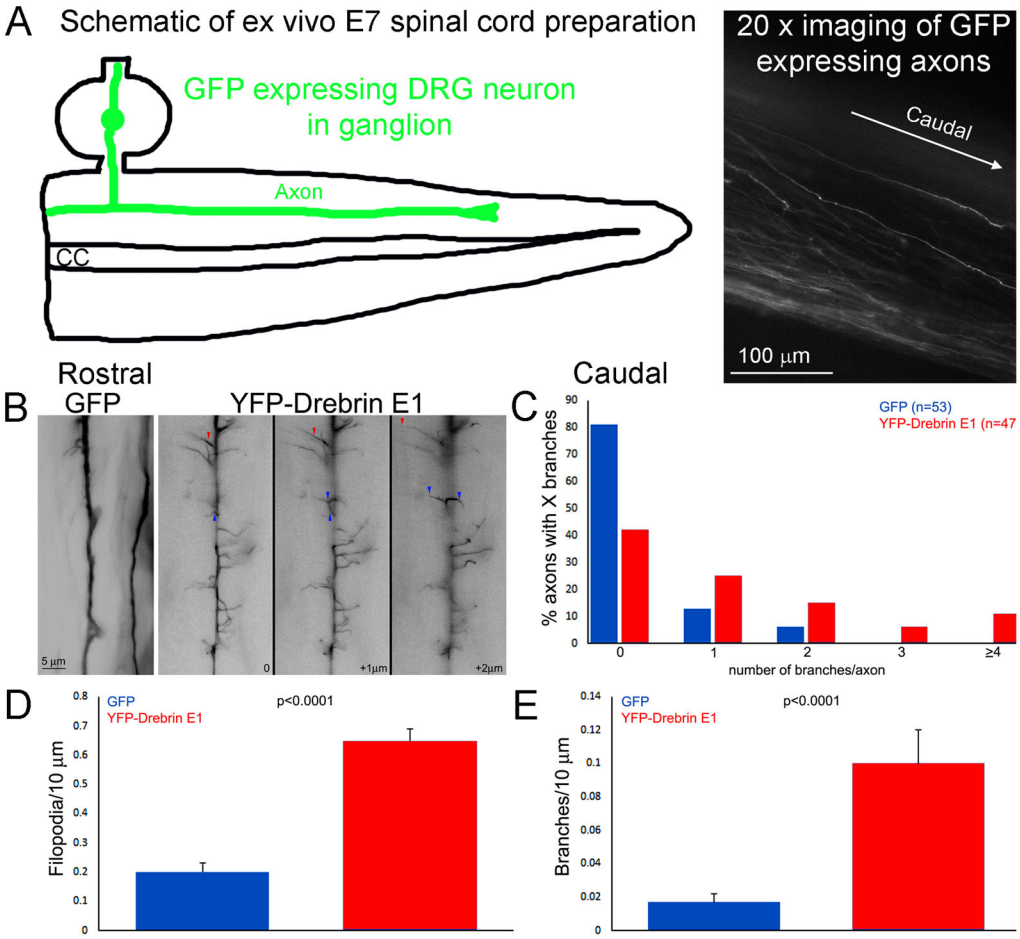

Figure 2.

In ovo expression of drebrin E1 in dorsal root ganglion sensory neurons affects the morphology of their axons in the spinal cord. **(A)** Schematic showing the ex vivo E7 spinal cord following dissection and placement in a video imaging dish. The right panel shows an example of GFP expressing axons imaged at 20x from an ex vivo spinal cord. For additional details and examples of the ex vivo system readers are directed to Spillane et al (2011) and Spillane et al (2012). **(B)** Examples of GFP control and YFP-drebrin E1 expressing sensory axons in the dorsal spinal cord. In ovo transfection was performed at embryonic day 3 and spinal cords harvested and imaged live at 100x at day 7 (as in Spillane et al., 2011, 2012). The control axons exhibit a simpler morphology than the drebrin expressing axons. The drebrin expressing axons exhibited numerous filopodia and branches which extended dorsal and ventral into the cord. Three focal planes are shown for the drebrin expressing axon with + μm representing more ventrally positioned planes. The red and blue arrowheads track examples of processes projecting through the planes. **(C)** Distribution of axons with X branches in the spinal cord (n=53 and 47 axons for GFP and YFP-drebrin E1 from 3 and 4 spinal cords, respectively). **(D–E)** Graphs showing the quantification of the number of filopodia (C) and branches (D) per unit length of axons in the spinal cord.

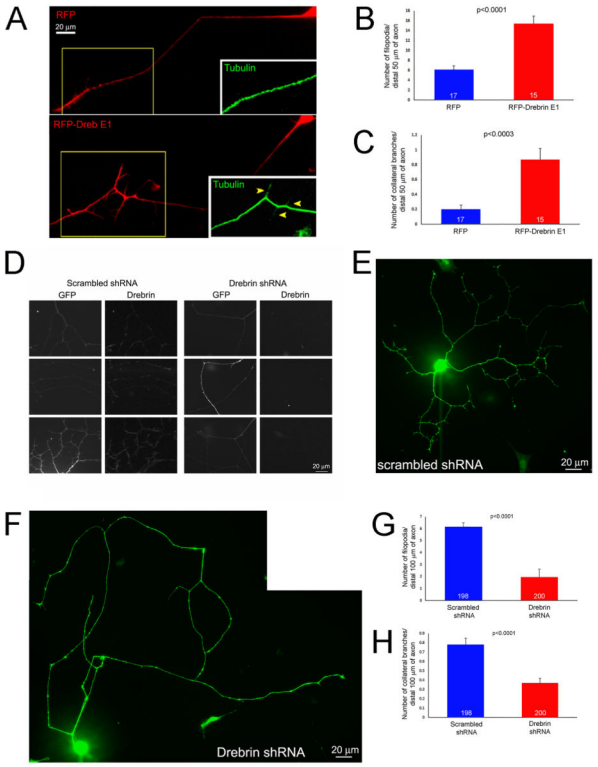

Figure 3.

Effects of drebrin E1 overexpression and shRNA-mediated depletion on axonal morphology. **(A)** Examples of the axons of cultured sensory neurons expressing RFP (control) or RFP-drebrin E1 at 24 hrs post-transfection. Drebrin expressing axons exhibited more filopodia and branches. The insets show tubulin staining for the boxed in regions. The RFP-drebrin branches contain tubulin staining, as expected for mature branches. **(B)** Quantification of the number of filopodia along the distal axons of RFP or RFP-drebrin E1 expressing neurons. Welch t-test. In all quantitative panels the sample sizes, axons, are denoted in the bars. **(C)** Quantification of the number of branches along the distal axons of RFP or RFP-drebrin E1 expressing neurons. Mann-Whitney test, medians of 0 and 1 respectively. **(D)** Examples of the efficacy of shRNA-mediated depletion of endogenous drebrin as detected by immunocytochemistry. Neurons expressing scrambled control shRNA contain detectable levels of drebrin along their axons. In contrast, by 3 days post transfection the axons of neurons expressing drebrin shRNA contain barely detectable drebrin, using identical imaging parameters. **(E and F)** Examples of the whole cell morphology of neurons cultured for 3 days following transfection with vectors expressing scrambled shRNA (E) and drebrin shRNA (F), the GFP-reporter signal is shown. **(G)** Quantification of the number of filopodia along distal axons in scrambled and drebrin shRNA expressing neurons. Welch t-test. **(H)** Quantification of the number of branches along distal axons in scrambled and drebrin shRNA expressing neurons. Mann-Whitney test, medians of 1 and 0 respectively.

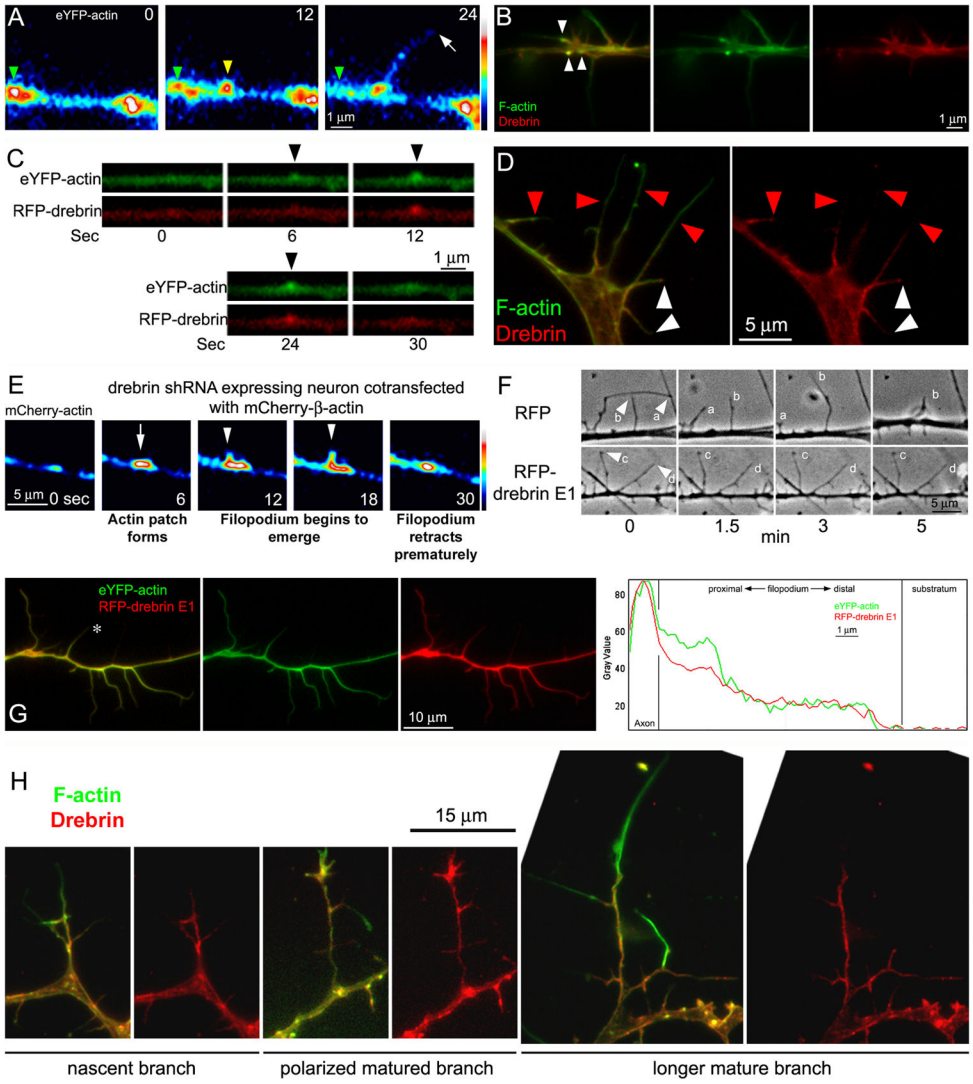

Figure 4.

Regulation of actin patches and the emergence and stability of filopodia by drebrin. **(A)** Examples of axonal actin patch dynamics. Time is shown in seconds in panels. The patch present at 0 sec (green arrowhead) undergoes dissipation by 24 sec. A new patch is formed between 0–12 sec (yellow arrowhead) and a filopodium emerges from it between 12–24 sec (white arrow at 24 sec). **(B)** Immunocytochemistry to detect endogenous drebrin and actin filaments (F-actin; phalloidin staining). Endogenous drebrin localized to axonal actin patches (white arrowheads). **(C)** Example of a time-lapse sequence imaging eYFP-β-actin and RFP-drebrin E1 in an axon during the formation and development of an actin patch (arrowheads at 6–24 sec). **(D)** Immunocytochemical localization of endogenous drebrin along filopodial shafts (also see panel B). The red arrowheads denote the distal most localization of drebrin along filopodial shafts exhibiting partial coverage by drebrin. The white arrowheads denote filopodia which contain drebrin throughout the shaft. As noted in the text, note that longer filopodial exhibit partial drebrin coverage. **(E)** Example of a time-lapse sequence of mCherry-β-actin in an axon co-transfected with the drebrin shRNA vector

(not shown). An actin patch forms at 6 seconds (arrow), and a “filopodial bud” begins to emerge at 12 sec (arrowhead) but only attains a short length before being resorbed into the patch (18–30 sec). **(F)** Examples of filopodial dynamics along the axons of control (RFP expressing) and RFP-drebrin E1 over-expressing neurons. The filopodia of the control axon exhibit bouts of elongation (filopodium b min 1.5–3) and retraction (filopodium a 0–5 min; filopodium b 3–5 min). In contrast, the filopodia of axons expressing RFP-drebrin E1 are much more stable (note that filopodia c,d undergo minimal to no change in length between 0–5 min). **(G)** Example of the distribution of RFP-drebrin E1 in an axon co-transfected with eYFP-β-actin. Note that the filopodia contain RFP-drebrin E1 throughout their length. Representative line scan analysis of the levels of actin and drebrin along the filopodium denoted by * is also shown in the rightmost panel. **(H)** Examples of drebrin localization in branches at different stages of morphological maturation.

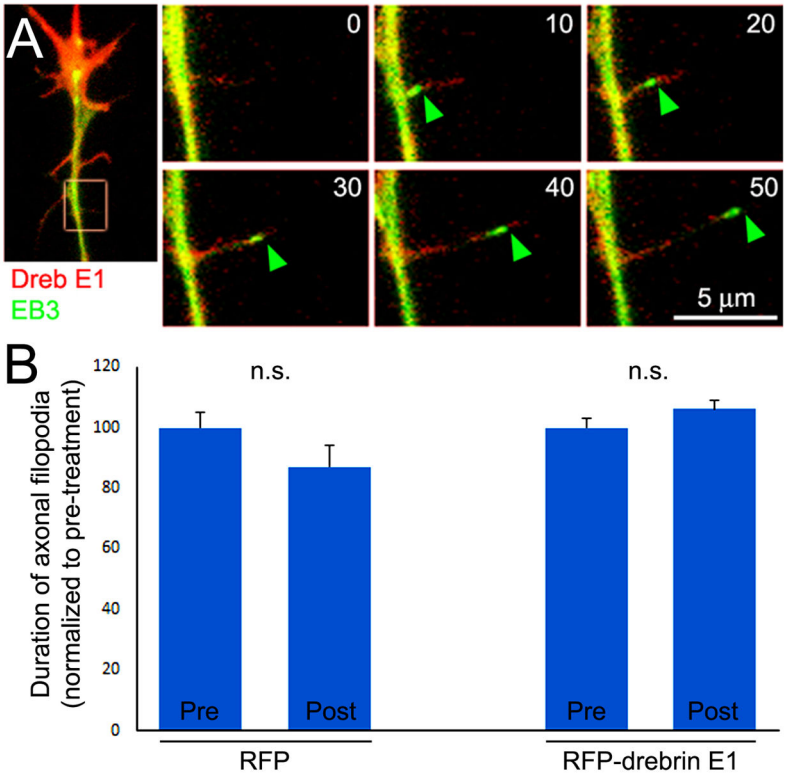

Figure 5.

Drebrin promotes the targeting of microtubule plus tips into axonal filopodia which is not required for drebrin-mediated stabilization of filopodia. **(A)** Example of GFP-EB3 imaging in an RFP-drebrin E1 expressing neuron. The leftmost panel shows the distal axons and the boxed in region denotes the subsequent panels reflecting stills from the timelapse (time shown in seconds in panels). An EB3 comet enters the filopodium at 10 sec and extends to the tip of the filopodium by 50 sec. **(B)** Analysis of the duration of axonal filopodia pre and post a 30 min treatment with 3 nM vinblastine, which as described in the text minimizes the entry of EB3 comets into filopodia in both RFP and RFP-drebrin E1 expressing neurons. The data are normalized to the pre-treatment condition for both groups (RFP and RFP-drebrin E1 expressing neurons; n=7 and 12 respectively). Vinblastine treatment did not affect the duration of filopodia in either group.

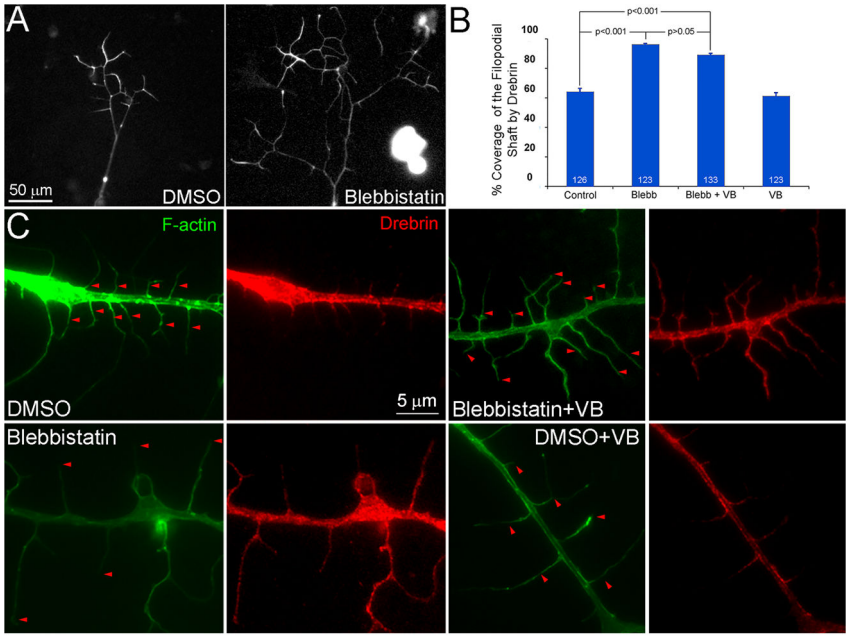

Figure 6.

Myosin II inhibition further promotes branching along the axons of RFP-drebrin E1 expressing neurons and results in the redistribution of endogenous drebrin along the distal shaft of axonal filopodia. **(A)** Note that the axon treated for 30 min with the myosin II inhibitor blebbistatin (50 μM) exhibits more branches and the branches are along longer, as detailed and quantified in the text. The RFP-channel, reflective of drebrin, is shown in both images. **(B)** Quantification of the percentage of coverage exhibited by drebrin along the shafts of axonal filopodia (0%=no drebrin extending into the filopodial shaft from the axon, 100%=drebrin found from the base to the tip of the filopodium). Number of filopodia sampled is shown in the bars. Treatment with vinblastine (VB) alone did not affect the distribution of drebrin relative to control DMSO treatment alone (p=0.39). **(C)** Examples of the intra-filopodial distribution of drebrin in DMSO and blebbistatin treatments ± treatment with VB. Note that in blebbistatin treated axons drebrin localizes along the majority of the filopodial shaft and that treatment with VB does not alter this distribution as reflected by the quantification in panel B. As in Figure 3D, in the F-actin panels the red arrowheads denote the distal most extent of drebrin localization in respective filopodia.

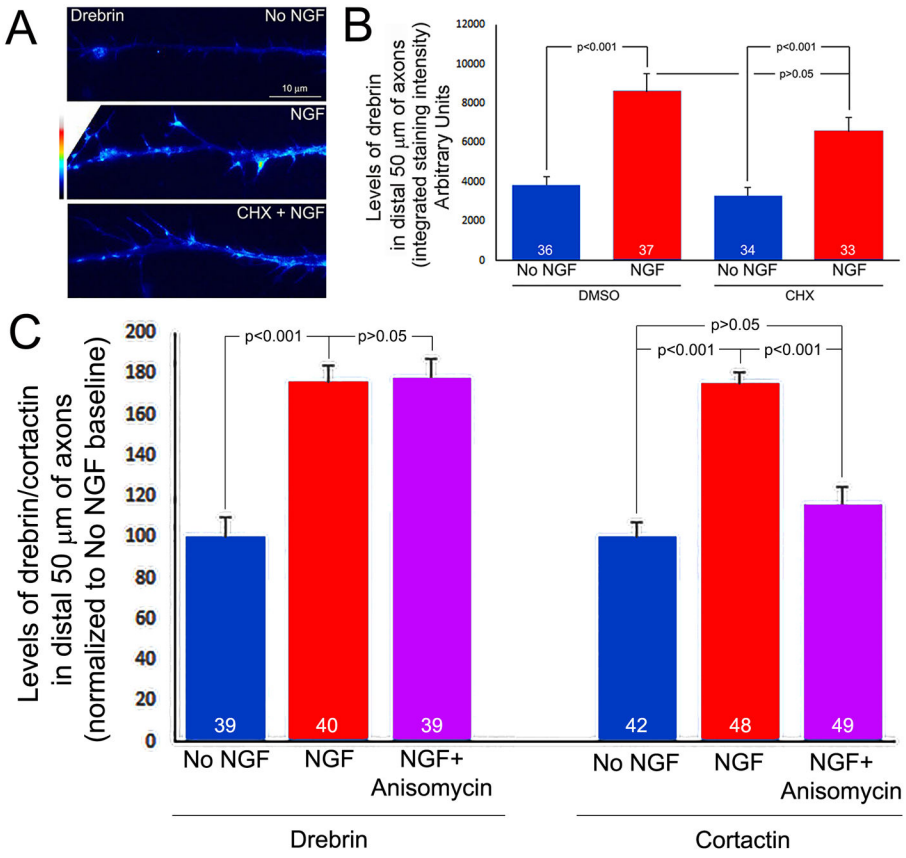

Figure 7.

NGF increases the axonal levels of drebrin in a cycloheximide and anisomycin insensitive manner. **(A)** Images of endogenous drebrin detected through immunocytochemistry and false colored to reveal relative levels. All images were acquired with identical parameters. A 30 min treatment with NGF increased the levels of drebrin, and the increase was not affected by treatment with cycloheximide (CHX, 35 µM). **(B)** Quantification of the total integrated intensity in distal axons as a function of NGF and CHX treatments. NGF increased the levels of drebrin in a manner insensitive to CHX treatment. CHX treatment alone did not affect baseline levels of drebrin. **(C)** Quanitification, as in panel B, of drebrin and cortactin levels following a 30 min treatment with NGF ± anisomycin (40 µM, 15 min pretreatment).

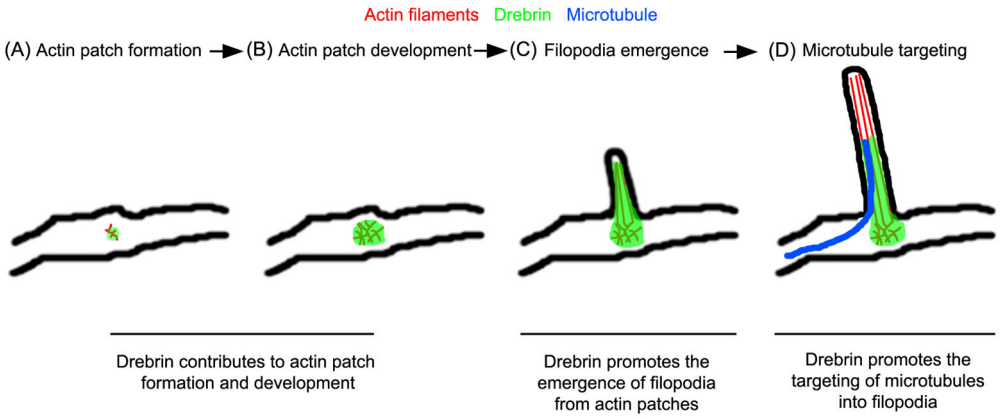

Figure 8.

Model of the spatio-temporal functions of drebrin in the coordination the cytosketon during the formation of axon collateral branches. The image depicts the first two phases of axon collateral branching, the formation of axonal filopodia (A–C) and the targeting of microtubules into filopodia (D). (A–B) Drebrin targets to axonal actin patches and is required, but not sufficient, for their formation and development. The observation that actin patches that form in the presence of drebrin shRNA exhibit greater durations indicates that drebrin may also control the turnover of filaments in patches. (B–C) Drebrin is involved in the formation of a filopodial bundle of actin filaments from actin patches, a role possibly mediated through the regulation of other actin binding proteins, as discussed. Drebrin also serves to stabilize filopodia after their formation. (D) The localization of drebrin to actin patches and the proximal segment of the associated filopodia promotes the entry of microtubule plus tips into filopodia, priming the filopodium for maturation into a collateral branch.